

Estimation of proton profile on rear surface of the target where ultraintense laser focused

Y. Oishi¹, T. Nayuki¹, T. Fujii¹, Y. Takizawa¹, X. Wang¹, A.A. Andreev^{1,2}, K. Horioka³,
T. Yamazaki¹ and K. Nemoto¹

*1. Central Research Institute of Electric Power Industry, 2-11-1, Iwado kita, Komae-shi,
Tokyo 201-8511, Japan*

2. Research Institute for Laser Physics, 12, Birzhevaya Line, St. Petersburg 199034, Russia

*3. Interdisciplinary Graduate School of Science and Engineering, Tokyo Institute of
Technology, 4259, Nagatsuta-cho, Midori-ku, Yokohama 226-8502, Japan*

1. Introduction

High-energy ion production by the irradiation of ultrashort laser pulses on a thin film is currently an attractive issue because of the potential applications [1]. Regardless of the target material, the most predominantly accelerated ion is the proton because of its small mass. The source of protons is thought to be contaminated layers on the target surface, and the force for proton acceleration is thought to be produced by the plasma sheath at the surface of the target [2-4]. The measurement of the proton profile on the target surface can be very useful for studies on the acceleration mechanism of protons and leads to engineering applications, such as an increase in ion yield and improved directivity of ion beams. Recently, some groups have reported the proton beams profiles using penumbral imaging technique [5], direct surface imaging [6] and periodically structured test objects [7]. Here, we propose another method of estimation of the proton source size on the rear surface of a target using a Thomson mass spectrometer and report experimental results using this method.

2. Theory

The key point is that placing a pinhole between the target and a proton detector like a pinhole camera. However, the pinhole diameter is usually comparable to or larger than the ion source size. Thus, a numerical procedure is necessary to retrieve the ion source profile from the ion pattern obtained on the observing plane. Figure 1 shows a schematic drawing of the coordinates for calculation. $f(x,y,E)$, $g(X,Y,E)$, and $g'(Y',E)$ are proton density profiles on the rear surface of the target, on the detector without the Thomson mass spectrometer, and on the detector with the Thomson mass spectrometer, respectively. Here, we consider one-dimensional profiles $f(y,E)$, $g(Y,E)$, and $g'(Y',E)$ for simplicity. These are all functions of the proton energy E . l_1 is the distance from the target to the pinhole, l_2 is that from the pinhole to the detector, while r_{ph} is the pinhole radius. $f(y,E)$ and $g(Y,E)$ satisfy

$$g(Y, E) = \int \frac{f(y, E)h(y, Y)}{2(l_1 + l_2) \tan \theta_c} dy \quad (1)$$

The denominator is derived from particle number conservation, when it is assumed that the protons are emitted homogeneously in a cone angle of θ_c (half angle). $h(y, Y)$ determines whether protons at y can reach Y on the detector, and depends on r_{ph} , l_1 , l_2 , and θ_c . In our experiment, these values are $r_{ph} = 25 \mu\text{m}$, $l_1 = 17\text{cm}$, $l_2 = 13\text{cm}$, and $\theta_c = 20$ degree for $E > 100$ keV. We assume that θ_c is proportional to $E^{-0.5}$ based on ref. [4]. Protons generated at (x, y) can reach (X, Y) , only when two restriction (i) the line connecting y and Y is not obstructed by the pinhole plate, and (ii) the angle between the line and the line normal to the target surface is less than θ_c are satisfied. Next, the transfer from $g(Y, E)$ to $g'(Y', E)$ by the Thomson mass spectrometer should be considered. Protons with energy E_o are transferred at approximately $(X_{E_o}, Y_{E_o}) = (k_X/\sqrt{E_o}, k_Y/E_o)$, where k_X , k_Y are the Thomson mass spectrometer constants. The l_2 in eq. (1) should be replaced by $l_2 + \sqrt{(X_{E_o})^2 + (Y_{E_o})^2}$ because the distance between the pinhole and transferred point depends on E . Since $f(y, E)$ has an area, protons with energies $E_o \pm \Delta E$ also reach approximately (X_{E_o}, Y_{E_o}) and overlap. However, we consider one-dimensional case here, we can ignore the overlap effect. Thus, $g'(Y', E)$ is obtained just replacing l_2 in $g(Y, E)$ to $l_2 + \sqrt{(X_{E_o})^2 + (Y_{E_o})^2}$. Finally, a Gaussian profile, such as $f(y, E) = a(E) \exp(-y^2/b(E)^2)$, is assumed and parameters which best fit the experimental result $g'_{exp}(Y', E)$ should be found by calculating eq. (1).

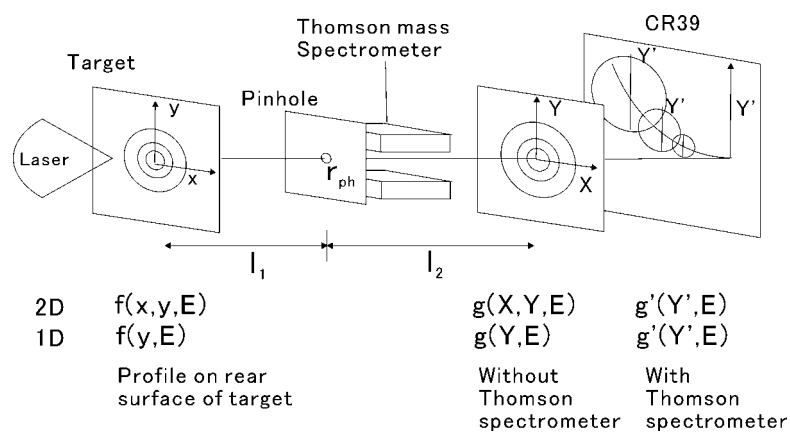


Fig. 1 Schematic drawing of the coordinates for theory

3. Experiments

The experiments were carried out using a Ti:Al₂O₃ laser (THALES LASER, Alpha 10/US-20TW) and is able to deliver up to 1 J, 50-fs pulses at a fundamental wavelength of 800 nm. In this study, the delivered energy to the experimental chamber was 220 mJ, the pulse

duration was 55 fs. The p-polarized laser beam was focused using a f/3 off-axis parabolic mirror, and was incident at an angle of 45 degree to the target surface. The focused spot on the target included coma aberration and the size of the main spot on the target was $4 \times 11 \mu\text{m}^2$ in full width at half maximum (FWHM), which included approximately 55% of the total energy. Therefore, the laser energy focused on the main spot was estimated to be 120 mJ, which led to $I = 6.6 \times 10^{18} \text{ W/cm}^2$. A thin copper tape of $5 \mu\text{m}$ thickness was used as the target [8], and was translated for every shot so that a fresh surface was irradiated. The energy spectra of protons ejected perpendicularly from the target surface at the opposite side of the laser irradiation were measured using the Thomson mass spectrometer. The electric and magnetic fields of the spectrometer were $3.3 \times 10^5 \text{ V/m}$ and 5.1 k Gauss, respectively. The deflection length by the fields was 4.5 cm. A $50 \mu\text{m}$ pinhole was located in front of the

Thomson mass spectrometer. A nuclear track plate CR39 located 10 cm from the center of the deflector was used as an ion detector. The tracks on the CR39 were observed with an optical microscope and a 16-bit charged coupled device (CCD) camera after etching for 6 hours in a 6.25 N, 70 degree NaOH solution. The number of accumulated laser shots was 50.

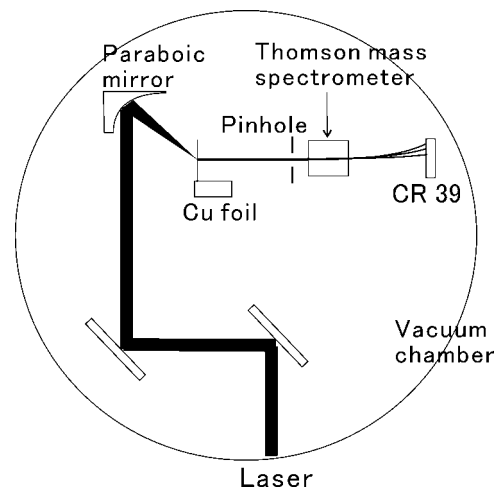


Fig. 2 Schematic drawing of the experimental layout

4. Results and Discussions

The process to obtain $g'_{exp}(Y', E)$ was three steps. (i) CCD image was divided into 61 box of 8 pixels each in the Y' direction. (ii) Etched pits in each box which consists of 432×8 pixels ($600 \times 11.1 \mu\text{m}^2$) were counted and 61 array data for each E were obtained. (iii) The counting numbers per X' were converted to $g'_{exp}(Y', E)$ per keV. Figure 3 shows the dependences of proton source size D_p (FWHM) on E . Here, we also plotted two-dimensional results, which were obtained by using $f(x, y, E)$ and $g(X, Y, E)$ instead of $f(y, E)$ and $g(Y, E)$, and by considering overlap effect which occurs in the transfer from $g(X, Y, E)$ to $g'(Y', E)$ by the Thomson mass spectrometer. More detail process will be described elsewhere. Two-dimensional results are a

little lower than one-dimensional, but the differences are not so significant. We should pay attention to the fact that D_p is not constant, such as $150\ \mu\text{m}$ at $E=400\ \text{keV}$ and $70\ \mu\text{m}$ at $E=1.1\ \text{MeV}$. The slope change of D_p at approximately $E=400\ \text{keV}$ is particularly large. Two or more temperatures in proton spectra observed thus far

[9,10] might be related with the slope change of D_p . Furthermore, D_p is larger more than 7 times of the laser spot size of $4\times 11\ \mu\text{m}^2$, which is close to M. Roth *et al.*'s [6] and M. Borghesi *et al.*'s [7] reports. The force for proton acceleration is thought to be produced by the plasma sheath at the surface of the target and during the acceleration processes, the regime of proton acceleration should be spread.

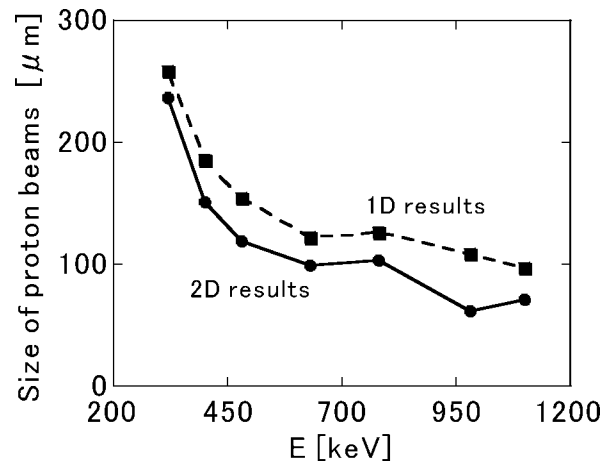


Fig. 4 Dependences of source size of proton beams on E .

4. Summary

In summary, we proposed and conducted the measurement of the energy-resolved source profile of proton beams on the rear surface of a target using a Thomson mass spectrometer. The source size of the proton beams on the target was found to be energy dependent: Typical beam sizes in FWHM were $150\ \mu\text{m}$ at $E=400\ \text{keV}$ and $70\ \mu\text{m}$ at $E=1.1\ \text{MeV}$.

References

- [1] D. Umstadter, J. Phys. D: Appl. Phys. **36** R151 (2003) and references therein.
- [2] E.L. Clark, *et al.*, Phys. Rev. Lett. **84**, 670 (2000).
- [3] R.A. Snavely, *et al.*, Phys. Rev. Lett. **85**, 2945 (2000).
- [4] Y. Murakami, *et al.*, Phys. Plasmas **8**, 4138 (2001).
- [5] M. Zepf, *et al.*, Phys. Plasmas **8**, 2323 (2001).
- [6] M. Roth, *et al.*, Plasma Phys. Controlled Fusion **44**, B99 (2002).
- [7] M. Borghesi, *et al.*, Phys. Rev. Lett., **92**, 055003-1 (2004).
- [8] T. Nayuki, *et al.*, Rev. Sci. Instrum. **74**, 3293 (2003).
- [9] I. Spencer, *et al.*, Phys. Rev. E. **67**, 046402-1 (2003).
- [10] T. Fujii, *et al.*, Appl. Phys. Lett. **83**, 1524 (2003).